A TEMPERATURE AND MOISTURE MODULE FOR HYDRATING PORTLAND CEMENT CONCRETE PAVEMENTS

Jin-Hoon Jeong, Ligang Wang, and Dan G. Zollinger, Ph.D. PE
Department of Civil Engineering, Texas A&M University
College Station, Texas 77843-3136, U.S.A.

A computer based temperature and moisture analysis module has been recently developed at the Texas Transportation Institute referred to as Temperature and Moisture Analysis for Curing Concrete ($TMAC^2$). This module produces the moisture and temperature profiles and accounts for the interaction between them at any points in a hydrating concrete slab as a function of time and ambient boundary conditions. These profiles, which are transient in nature and determined as a function of curing methodology and material characteristics, can be easily transmitted to analytical software for stress and deformation evaluation. A special test slab was constructed and carefully instrumented for temperature and relative humidity monitoring to collect specific data for program verification purposes. Deflection data collected from the test slab were compared to the results from Westergaard type solution for corner displacement to show potential for pavement design application under a board set of condition depicted by temperature and moisture gradient prediction from the $TMAC^2$ software. This paper presents the details of the development of $TMAC^2$, verification of the analysis module, and examples of the effects of combinations of climatic, construction, and material factors on profile development. Details of the test slab and the instrumentation are also presented.

INTRODUCTION

In recent years, materials research in concrete has shown that control cracking in concrete pavements has become an issue of great concern. It has been found that the development of both temperature and moisture changes in a concrete slab in the first few days after the concrete has been placed are factors of early age restraint stresses and environmentally induced cracking which ultimately influence the performance of the slab over its lifetime (1-4). The knowledge of heat and mass transfer in terms of the prediction of temperature and relative humidity as a function of time and key material properties is thus important to the understanding of the curing effectiveness and cracking potential.

Figure 1 shows a typical temperature and stress development for the early stages of concrete hardening. During the first few hours after placing, compressive stresses due to volumetric expansion develop and are small because the Young's modulus is still low and the relaxation is high. When the peak temperature is exceeded, the remaining compressive stress decreases rapidly due to a temperature decrease. Thus, the concrete reverts to a stress-free condition at a temperature that is referred to as T_{zero} which is typically only a few degree below the peak temperature. Upon the further cooling, relatively high tensile stresses develop because of the increase in the Young's modulus of concrete and diminishing relaxation. As a result, tensile stresses increase and the potential for cracking increases. The thermally-induced stress has a function of the temperature variation below the set temperature of the concrete, depend upon the concrete modulus and the coefficient of thermal expansion (CTE). The CTE of concrete has

been shown to be a function of moisture content (1). It is important to characterize the distribution and history of pore humidity in order to achieve to the realistic estimation of concrete thermal expansion, strength, maturity and curing efficiency at various ages. Thus, in this respect, the characterization of key moisture-sensitive material properties constitutes a major component of determining the cracking tendency of concrete pavement.

The prediction of the temperature and moisture history and distribution in hardening concrete is also of great interest during construction for reasons such as: crack control and sawcut timing, assessment of curing effectiveness, and evaluation of the concrete strength development. These quality control procedures are often impacted by the effects of ambient weather conditions on the rate of strength-gain or hydration of the concrete mixture. In actual construction projects, fresh concrete is subject to many environmental changes in the process of hardening. Consequently, it would be advantageous to have analytical models that could be used to estimate the state of concrete at any time during the curing cycle in terms of the environmental conditions that exist and the method of curing the concrete is subjected to.

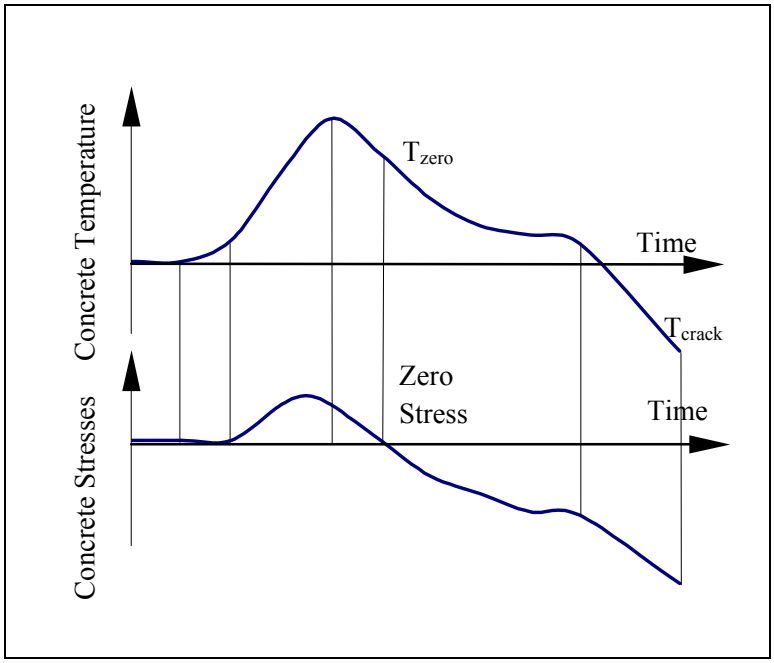

Figure 1 The Concrete Temperature and Stress Development with Time (5).

During the early age of concrete hardening, the hydration process plays a determinant role in the behavior of a concrete slab. However, the environmental conditions influence concrete temperatures and moisture conditions at the pavement surface. The hydration process generates internal heat, which influence the rate of chemical reactions of the cementitious materials and water. In order to evaluate the effects of the factors that effect the hydration process and its effect on early age slab behavior, temperature distributions of the concrete pavement are estimated by analyzing the transient heat transfer between the concrete and the surrounding condition as represented by the boundary value equations where the effects of environmental factors such as air temperature, wind velocity, solar radiation and heat of hydration are accounted for. Convection type heat transfer takes place where a concrete surface is exposed to an air steam caused by wind which is at a different temperature than that of the concrete pavement. The concrete surface is also affected by solar gain heat transfer which is transported by electromagnetic waves between the concrete surface and its surroundings. The rate at which heat is absorbed by a concrete surface is termed as solar radiation. On the other hand, vertical moisture distributions within a concrete pavement are estimated by analyzing the transient mass transfer between the concrete and the surroundings as represented by boundary value equations

where the effects of environmental factors such as air relative humidity are accounted for. These boundary interactions are typically analyzed by use of the finite element method. Since in-situ temperature prediction depends on a thermal distribution model at early concrete ages, the heat of hydration must also be considered in the program to accurately estimate temperature distributions of concrete pavement during the early stages of hydration.

MODELS FOR TEMPERATURE AND MOISTURE PREDICTION

Concrete pavement performance data suggests that prediction of the distribution and history of temperature and relative humidity in concrete pavement should be of major importance to the construction industry. Its prediction is necessary for an estimation of drying shrinkage, thermal expansion and strength. Temperature and moisture gradients in young concrete are primary contributors of crack formation. Consequently, a theoretical basis for the simultaneous modeling of heat transfer and moisture loss during concrete hardening is discussed. The transport models for heat transfer and moisture loss are formulated in a way that includes all pertinent heat and mass transfer mechanisms and ambient boundary conditions. The finite element method is employed to give numerical solutions. The governing equation for moisture mass transfer is a time-dependent partial differential equation as that for heat transfer. However, they are different from one another in that,

(1) The heat (Q_h) generated from hydration that produces additional internal heat appears in the heat transfer governing equation, while no similar moisture term appears in the drying processes,
(2) The moisture diffusivity (D) depends upon the relative humidity (H) and thus varies with time in the drying process, while the thermal conductivity does not change with ambient temperature (but should as a function of moisture), and
(3) The boundary conditions of the moisture mass transfer equation are much more complex than those of the heat transfer governing equation and must be treated independently.

Governing Equations of Heat Transfer and Moisture Diffusion

The two dimensional governing equation of heat transfer for temperature prediction in a early age concrete pavement taking heat of hydration and ambient temperature conditions into account is (6,7):

$$\frac{\partial}{\partial x}\left(k_x \frac{\partial T}{\partial x}\right) + \frac{\partial}{\partial y}\left(k_y \frac{\partial T}{\partial y}\right) + Q_h(t,T) = \rho c_p \frac{\partial T}{\partial t} \qquad (1)$$

where,

T = temperature in concrete pavement (^oC),
t = time (hr),
x, y = depth and longitudinal coordinates in concrete pavement (m),
k_x, k_y = thermal conductivities of concrete in x and y directions ($W/m/^oC$),
ρ = concrete density (kg/m^3),
c_p = specific heat ($J/kg/^oC$), and

Q_H = generated heat from heat of hydration of cement and external sources (W/m^3).

The thermal parameters in Equation (1) are basic material properties determined by select laboratory and ASTM test procedures that are not elaborated here.

Diffusivity is important in modeling moisture flow in hardening concrete. At a constant water content (w), diffusivity changes little with time in hardened concrete though it changes greatly during the first 24 hours after placement of concrete. Diffusivity has been found to be a function of humidity, age of concrete, and porosity of cement paste. The rate of moisture flow through concrete can be expressed by the velocity of flow (J) representing the mass of evaporable water passing through a unit area perpendicular to the direction of flow per unit time. The velocity of flow by Darcy's law is derived from energy gradients:

$$J = -C \cdot grad\mu \tag{2}$$

where, μ is Gibb's free energy (GFE) per unit mass of evaporable water and C characterizes the permeability of the porous of concrete. The Equation (2) is restricted to small energy gradients and laminar flow conditions. Assuming water vapor behaves as an ideal gas, Gibb's free energy is (8):

$$\mu = (\frac{RT}{MV_w}) \cdot \ln h + \mu_{sat}(T) \tag{3}$$

where,

R = universal gas constant (8.3143 J/mol/^{o}K),
T = absolute temperature (^{o}K),
M = molecular weight of water (18.015 g/mol),
V_w = specific volume of water (1 cm^3/g),
h = relative humidity, and
μ_{sat} = μ when saturated.

Equation (2) can be rewritten in terms of relative humidity and temperature as:

$$J = -c \cdot gradh \tag{4}$$

where, the coefficient c is permeability as a function of temperature and humidity as below.

$$c = (\frac{RT}{MV_w}) \times (\frac{C}{h}) \tag{5}$$

The governing equation of moisture diffusion is derived from Equation (4) by introducing moisture isotherm concept, hygrothermic coefficient (K), and humidity at self-desiccation of a sealed sample (h_s) as:

$$\frac{\partial h}{\partial t} = D\frac{\partial^2 h}{\partial x^2} + \frac{\partial h_s}{\partial t} + K\frac{\partial T}{\partial t} \tag{6}$$

where, D is diffusivity (L^2/t), dh_s is change in relative humidity due to hydration at a constant water content and time, and K is hygrothermic coefficient representing the change in relative humidity due to one degree change in temperature

The linear diffusion mass transfer equation used extensively in the past is known to give a very poor fit of experimental data over certain period of time. Namely, as drying progresses, the remaining moisture is lost with ever increasing difficulty and drying becomes much slower than extrapolation of the initial drying curve that a linear diffusion theory would predict. This fact suggested that diffusivity decreases with water distribution. The relationship between D and h has been found to be (8):

$$D(h) = D_1\left[\alpha_0 + \frac{1-\alpha_0}{1+\left(\frac{1-h}{1+h_c}\right)^n}\right] \tag{7}$$

where,

D_1 = diffusivity of concrete at h=1 and
A_0, h_c, n = materials parameters of concrete.

The D(h) is a nonlinear function of the function h. In computation, D can be evaluated by updated h value of the last time step of the numerical program.

Boundary Conditions of Heat Transfer and Moisture Diffusion

The boundary conditions associated with a concrete pavement consist of conditions associated with both the pavement surface and bottom conditions. At the pavement surface, heat transfer is affected by all the heat mechanisms such as convection, solar gain, and solar radiation through the environment. At bottom of the concrete layer, heat transfer is affected by conduction according to the subbase thermal properties which listed in Equation (1). Similar to the boundary conditions in the subbase, heat transfer to the soil under the subbase is affected only by conduction and is dependent on the thermal properties of soil. These two conditions are summarized as follows:

$$-k\nabla T \cdot n + q_c + q_r - q_s = 0 \qquad \text{on pavement surface} \tag{8}$$

$$-k\nabla T \cdot n = 0 \qquad \text{on pavement bottom} \tag{9}$$

where,

k = thermal conductivity (W/m/^{o}C),
q_c = heat flux due to convection (W/m^3),
q_r = heat flux due to surroundings and sky (W/m^3),
q_s = solar radiation absorption (W/m^3),
∇ = gradient notation, and
n = unit direction of heat flow by vector notation.

Equation (6) represents the physical mechanism of moisture diffusion in a concrete pavement, with its surface subject to moisture evaporation. At the time when fresh concrete is placed, the concrete pavement is assumed to be completely wetted. The driving force of the moisture evaporation is the moisture difference between water inside concrete and ambient air. These boundary conditions and initial conditions are represented mathematically as:

$$E = \frac{Q\Delta + \gamma J}{\Delta + \gamma} \tag{10}$$

and

$$\Delta = \Delta_0 \left(\frac{C - L}{C}\right) \tag{11}$$

where,

E = evaporation (kg/m^2/hr),
Q = net radiation exchange (kg/m^2/hr),
γ = psychrometric constant (kg/m^2),
J = flow across the interface (kg/m^2/hr),
Δ_0 = slope of the saturation vapor pressure versus temperature at a given air temperature (kg/m^2),
L = effective curing thickness (cm), and
C = depth of ideal curing (=7.6 cm).

Coupling Effect between Temperature and Relative Humidity

Evaporation at the surface of concrete slab is defined as the net rate of vapor transport to the atmosphere. This change in state requires an exchange of approximately 600 calories for each gram of water evaporated. Vaporization removes heat from water near the surface of the concrete slab being vaporized. The latent heat of vaporization is the amount of heat absorbed by a unit mass of a water, without change in temperature, while passing from the water to the vapor state. The heat of vaporization of water (H_v) in calories per gram varies with temperature but can be determined accurately up to 40°C by (9):

$$H_v = 597.3 - 0.564T \tag{12}$$

where, T is the temperature in degrees Celsius. Therefore, movement of water effects to the changes in temperature of concrete slab near surface.

As shown in Equation (6), the change in relative humidity in concrete slab is affected by temperature. The governing equation of moisture diffusion contains a term expressed as the product of hygrothermic coefficient (K) and rate of temperature. The rate of temperature can be replaced by rate of relative humidity because the hygrothermic coefficient (K) represents the change in relative humidity due to on degree change in temperature at a constant water content and a given level of hydration.

KEY MATERIAL PROPERTIES AND EVALUATION

Key material properties that standout in the early age hardening process are concrete diffusivity and conductivity. For the back calculations of the concrete moisture diffusivity and thermal conductivity, a cylindrical concrete specimen with diameter of 20.3 cm (8 inch) and height of 30.5 cm (12 inch) was prepared. Temperature and moisture sensor locations were 2.5, 7.6, and 12.7 cm (1, 3, and 5 inch) below the exposed surface along the axis of the specimen.

Table 1 Mix Design for One-Dimensional Laboratory Temperature and Moisture Monitoring (5).

Material	Full-Size Batch Design
GH Servtex Limestone (Well Graded)	812 kg (1788 lb)
GH Jones Sand	535 kg (1178 lb)
Cement	256 kg (564 lb)
Water	104 kg (229 lb)
A/E Agent	6.00 oz-US
Water Reducer	27.00 oz-US

An axisymmetric mass transfer model was used for numerical analysis. The cylindrical specimen was discretized into the finite element mesh shown in Figure 2. There is total $6 \times 14 = 84$ elements with 377 nodal points (nine nodal points per element). The cartesian coordinates x, y of the rectangular elements coincide with the cylindrical coordinates r, z, respectively.

Back Calculation of Thermal Conductivity

The traditional method of measuring the thermal conductivity is a steady-state heat experiment in which all temperatures are allowed to come to equilibrium before the required measurements are made. This method has the disadvantage in that the time taken to reach thermal equilibrium may be inconveniently long, particularly for concrete materials with low conductivities. To obtain thermal conductivity from the use of a guarded-hot-plate apparatus, surface flux measurements are needed besides temperature measurements.

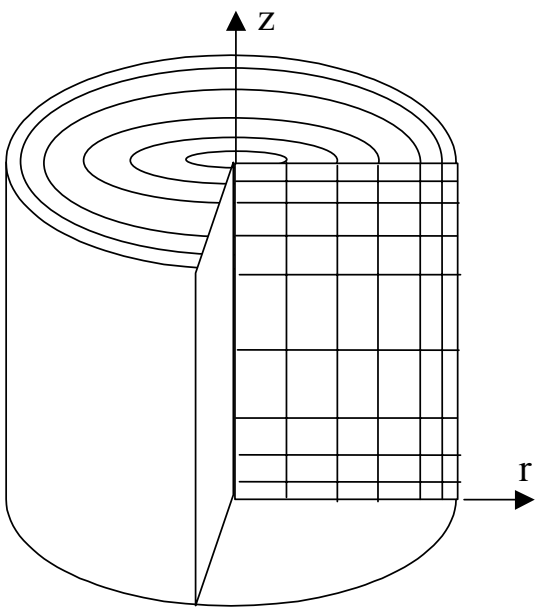

Figure 2 The Axisymmetric Model of the Contrete Cylinder and Meshes (5).

The thermal conductivities of concrete with degree of hydration were back calculated by use of the results from the laboratory temperature and moisture monitoring on the cylindrical specimen. The curves of temperature versus time and temperature versus vertical distance from the concrete surface were made and Equation (1), governing equation of heat transfer, was applied to back calculate the thermal conductivity from the curves. Heat of hydration, specific heat, and density of concrete were applied for the back calculation. Initially, the value of the thermal conductivity was recorded as 90 J/cm/hr/^{o}C as shown in Figure 3. The value of thermal

conductivity decreased as degree of hydration increased and was recorded as 45 J/cm/hr/^{o}C as the degree of hydration reached to 100%. Based on laboratory test results, concrete conductivity was 45(2-α) J/cm/hr/^{o}C where α being the degree of hydration and concrete specific heat as 0.89 J/g/^{o}C.

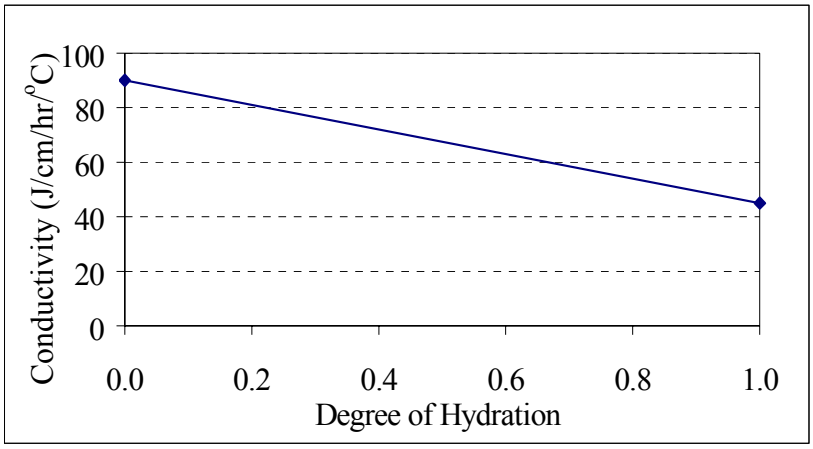

Figure 3 Concrete Conductivity Development versus Degree of Hydration (laboratory) (5).

The FEM code, TMAC[2], was also used to verify the fitness of the thermal conductivity back calculated from laboratory experiment to the analysis results from a numerical model. Concrete temperature at the three different depths (which are the same depths as for the experiments) were predicted using TMAC[2]. From the result, maximum temperatures occurred at 11.1 hours and were 37.6^{o}C at 2.5 cm (1 inch) below the concrete surface and 40.1^{o}C at 7.6 cm (3 inch) below the concrete surface and 42.3^{o}C at 12.7 cm (5 inch) below the concrete surface, respectively. The comparison between measured temperature and predicted temperatures was found to be satisfactory as shown in Figure 4.

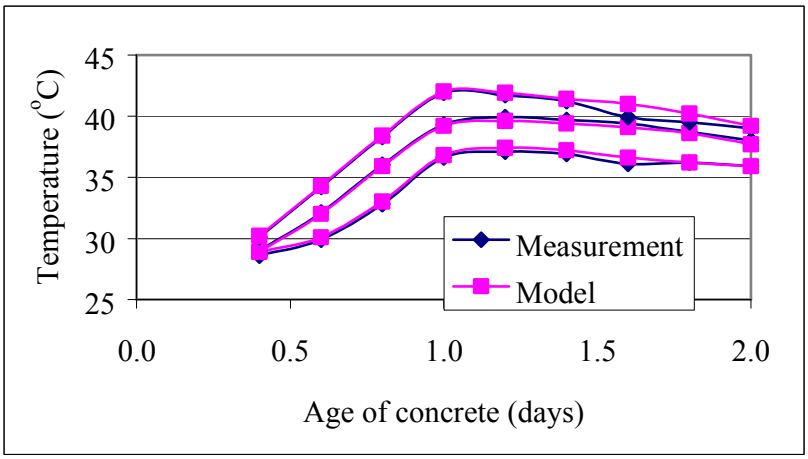

Figure 4 Comparison between Measured and Predicted Concrete Temperature History (Laboratory) (5).

Back Calculation of Moisture Diffusivity

The moisture diffusivities of concrete with time were back calculated by use of the results from the laboratory temperature and moisture monitoring. The curves of relative humidity versus time and relative humidity versus vertical distance from the concrete surface were made and Equation (4), governing equation of moisture diffusion, was applied to back calculate the diffusivity from the curves. The initial value of the diffusivity right after the concrete placement was 0.38 cm^2/day as shown in Figure 5. The value of diffusivity decreased exponentially with time and reached 0.24 cm^2/day at 2 days after the concrete placement.

The FEM code Temperature and Moisture Analysis of Curing Concrete (TMAC^2) was used to verify the fitness of the moisture diffusion back calculated from laboratory experiment to the analysis results from a numerical model. From the analysis by TMAC^2, it can be seen that the measured relative humidity 2.5 cm (1 inch) below the pavement surface drops from about 98% to 94% during the first 3 days of drying. The measured relative humidity 7.6 cm (3 inch) below the pavement surface drops from about 99% to 98% during the time. The measured relative humidity at 12.7 cm (5 inch) below the pavement surface keeps at about 100%, which indicates that moisture loss at this depth is negligible. The relative humidity were predicted to drop from 100% to 94% 2.5 cm (1 inch) below the pavement surface, while it were predicted to drop form 100% to 98% 7.6 cm (3 inch) below the pavement surface. The predicted relative humidity 12.7 cm (5 inch) below the pavement surface keeps at approximately 100% during the time. On the whole, predicted moisture profile corresponds to the measured data well.

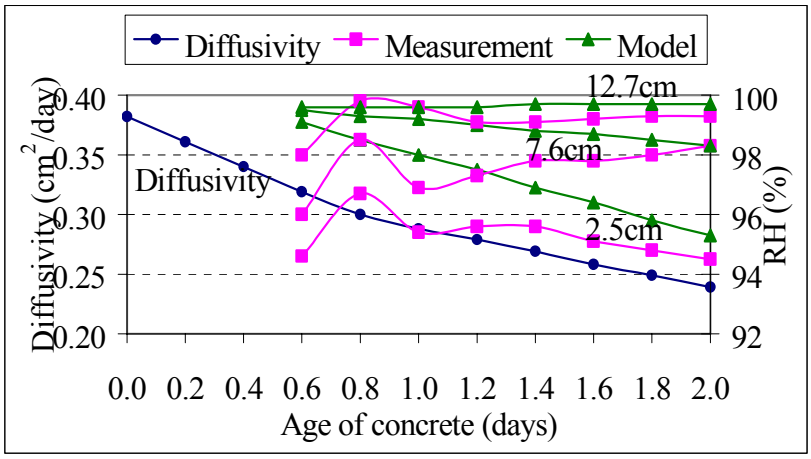

Figure 5 Moisture Diffusivity Development in Hardening Concrete (Laboratory) (5).

FIELD SLAB INSTRUMENTATION

The placement of a concrete slab was done at the Riverside Campus Annex test facility of the Texas A&M University, which is geographically located at College Station, Texas. Before placing the slab, a 10.2 cm (4 inch) thick lean subbase was placed. The subbase was 10.4 m (34 ft) in length and 4.3 m (14 ft) wide. The construction consisted of a 30.5 cm (12 inch) slab 9.2 m (30 ft) long and 3.7 m (12 ft) wide. The concrete mix design consisted of 6 sacks of Type I cement per 0.675 m^3 (cubic yard) with 20% of fly ash. The coarse aggregates were crushed limestone and the fine aggregates were natural sand. Field test indicated a water-cement ratio of 0.44, a 10.2 cm (4

Table 2 Mix Design and Characteristics in 0.765 m^3 (1 cubic yard) of Concrete (Test Slab).

Material	Proportions
Cement (type I)	221 kg (488 lb)
Fly Ash	56 kg (123 lb)
Fine Aggregate	508 kg (1120 lb)
Coarse Aggregate	840 kg (1852 lb)
Water	123 kg (271 lb)
Air Entrainer	1.35%
Water/Cement Ratio	0.44
Percentage of Coarse Aggregates	63%
Air Content	2.4%
Slump	17.8 cm (7.0 inch)
Unit Weight of Concrete	2286 kg/m^3 (142.73 lb/ft^3)

inch) slump and an air content of 2.4%. Table 2 shows the concrete mixture proportions

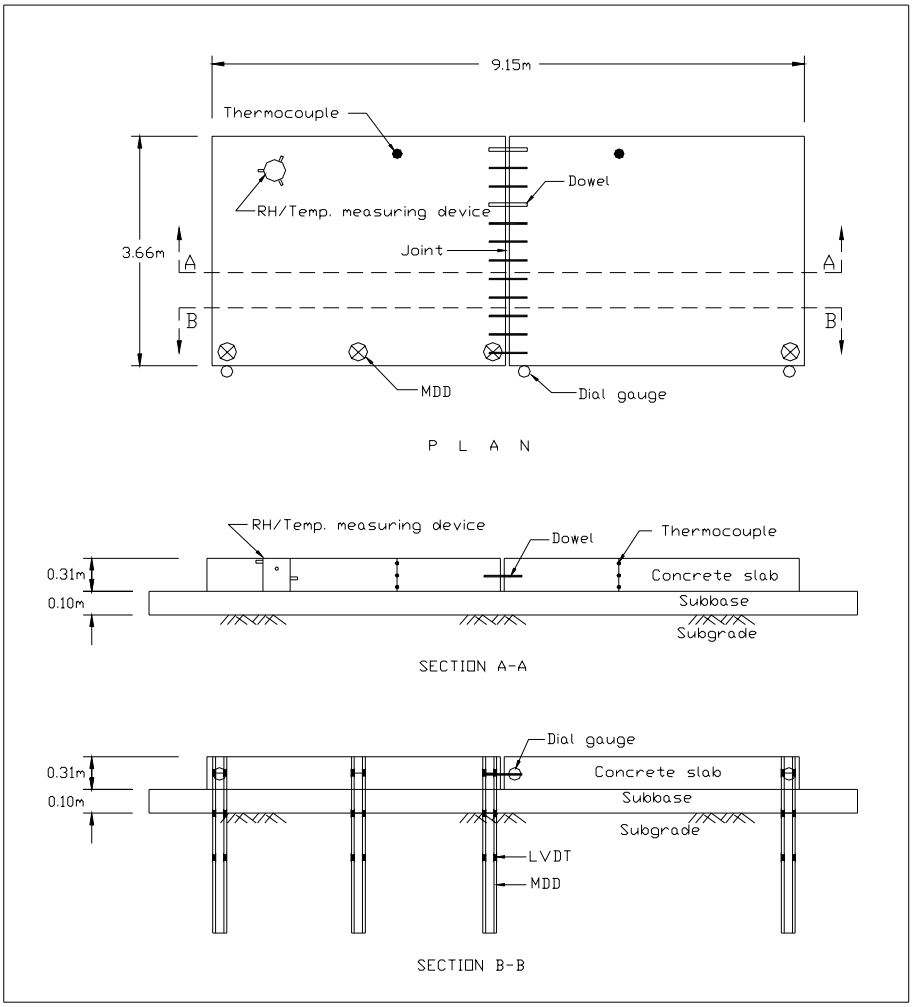

The slab instrumentation consisted of multiple depth deflectometers (MDDs), temperature and dew point measuring devices, thermocouples, dial gauges, and a Weather station. MDDs were placed within each layer of slab, subbase, and subgrade to collect vertical displacement data at critical positions noted in Figure 6. Temperature and dew point measuring devices were placed at different depths below the slab surface as shown in Figure 6. Thermocouples were installed to measure temperature profile within the slab. Also, to monitor the relative humidity and temperature condition immediately above the slab, four RH meters were positioned at various heights to collect evaporation related data. In order to obtain the general ambient weather conditions such as wind speed and direction, air temperature, solar radiation, rain fall, and so on, a local weather station was installed near the slab.

VALIDATION OF MOISTURE AND TEMPERATURE GRADIENT USING SLAB DATA

The measured temperature data show that the maximum temperature was generated between 6 and 7 hours after placement of concrete. 50.3^{o}C at 7.6 cm (3 inch) below the surface were recorded as maximum temperature of the slab. Overall temperature goes down from that point and the primary factor causing changes in temperature of slab is replaced from heat of hydration to weather condition as the rate of heat of hydration decrease. As maximum temperature goes down, the temperature is affected by air temperature mainly especially near the surface of slab. It is clear that the temperature profiles predicted by TMAC^{2} correspond to the temperature

profile measured in the field well as shown in Figure 7 for example. The predicted temperature through the slab profile is generally good although the variation of predicted temperature with time near the surface of the slab is larger than the variation of the measured temperature. But further adjustment in the boundary condition effects is warranted to improve the fit to the field results.

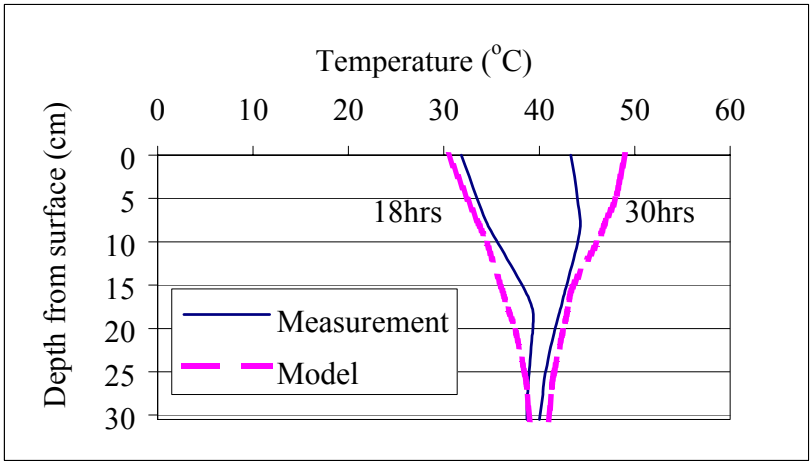

Figure 7 Comparison between Measured and Predicted Temperature Profile (Test Slab).

The measured relative humidity data show that the initial maximum relative humidity drops continuously from the next day morning of the concrete placement. The trend of relative humidity with time is affected by air relative humidity conditions especially near the surface of the slab. It was verified that the relative humidity profiles predicted by TMAC[2] fit the relative humidity profile measured for the test slab well near the surface of the slab as shown in Figure 8 for example. The predicted relative humidity is overestimated near the bottom of the slab. But the difference is may be due to self-desiccation effects.

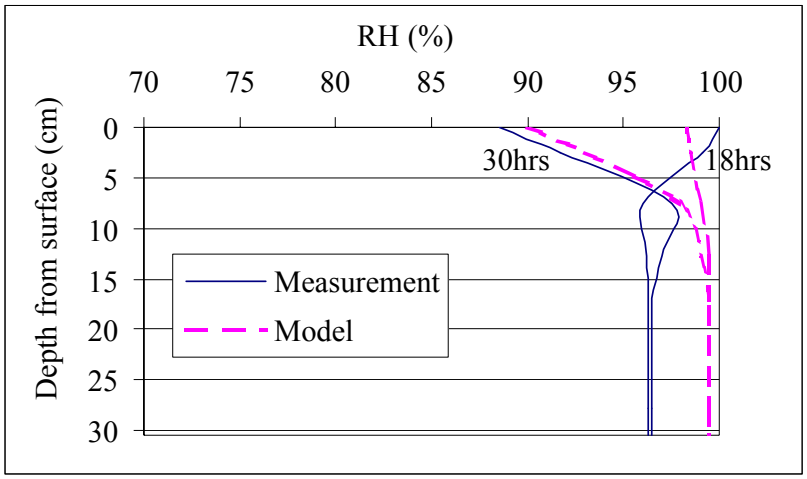

Figure 8 Comparison between Measured and Predicted Relative Humidity Profile (Test Slab).

APPLICATION OF PROFILE GRADIENTS TO DEFLECTION DEVELOPMENT

The temperature and relative humidity profile prediction from TMAC[2] can be applied to the prediction of behavior of concrete slab as a further validation measure. There already exist many solutions for the calculation of stress and deflection of slab due to temperature and moisture distribution. It is clear from the temperature and relative humidity profiles illustrated in Figure 7 and 8, that the change in temperature and relative humidity from top to bottom is not linear. In order to determine 'effective' temperature and relative humidity differences, the following

approach by Mohamed and Hansen (10) was used. A third degree polynomial function was used to represent the shape of the temperature or relative humidity differences vertically through the slab and is shown below:

$$\Delta T(z) = A + Bz + Cz^2 + Dz^3 \tag{13}$$

where, ΔT(z) is the temperature difference in temperature at a point at a given depth below the surface and the temperature at the bottom of the slab, and it can be replaced by the relative humidity difference $\Delta(1\text{-}RH^3)(z)$. The coordinate z is defined as zero at mid depth of slab where upward is negative and downward is positive. The equivalent nonlinear temperature difference can be expressed as:

$$\Lambda T_{eq} = -12\left(\frac{Bh}{12} + \frac{Dh^3}{80}\right) \tag{14}$$

where, h is thickness of concrete slab. The equivalent nonlinear relative humidity difference has the same equation as the Equation (14). The nonlinear temperature and nonlinear relative humidity differences with time from the test slab are illustrated in Figure 9. The day to day trends indicate that both the temperature difference and the relative humidity differences in slab would reach minimums in the morning and maximums in the afternoon. Where the equivalent relative humidity difference $\Delta(1\text{-}RH^3)_{eq}$ serves as same as the temperature difference ΔT_{eq} in the calculation of behavior of concrete slab.

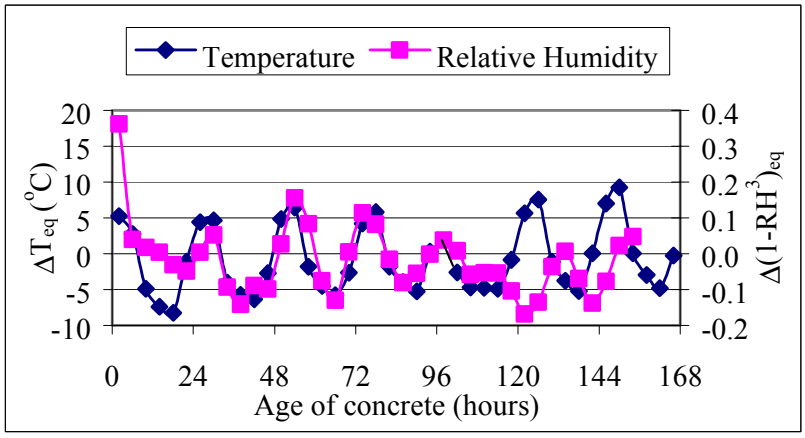

Figure 9 Equivalent Nonlinear Temperature and Relative Humidity Difference with Time (Based on Test Slab Data).

Corner deflection, the one of the main aspect of behavior of the concrete slab, can be calculated as shown in Equation (15). The result from the calculation is compared to the corner deflection data collected from the test slab to show that the predicted temperature and relative humidity profile can be used in the prediction of behavior of concrete pavement consequently (11).

$$w = (B_1 \cos y' \cosh y' + B_2 \sin y' \sinh y')(A_1 \cos x' + \sin x')e^{-x'} \tag{15}$$

where,

$$y' = \frac{y}{\sqrt{2}} \quad ,$$

$$x' = \frac{x}{\sqrt{2}} \quad ,$$

P = the radius of relative stiffness,
y = distance from slab corner along the transverse joint,
x = distance from slab corner along the longitudinal joint, and
A_i, B_i = function coefficients.

The solutions of the coefficient equations were developed depending whether the corner of the slab was in contact with the subgrade or base support as referred as lift-off and zero lift-off conditions (11).

Corresponding to this minimum peak of temperature and relative humidity differences shown in Figure 9, a upward corner deflection relative to a concave (curl up) slab configuration was measured at the test slab. On the other hand, the trend in temperature and relative humidity differences in the slab reached a maximum in the afternoon while downward corner deflection trends were investigated corresponding to a convex (curl down) slab configuration. The rain on the fifth day after construction caused the temperature and relative humidity differences in the slab to decrease. It is evident that this effect on the corner deflection persisted until the next morning as shown in Figure 10. The corner deflections calculated by Equation (15) agreed with the measured corner deflections well.

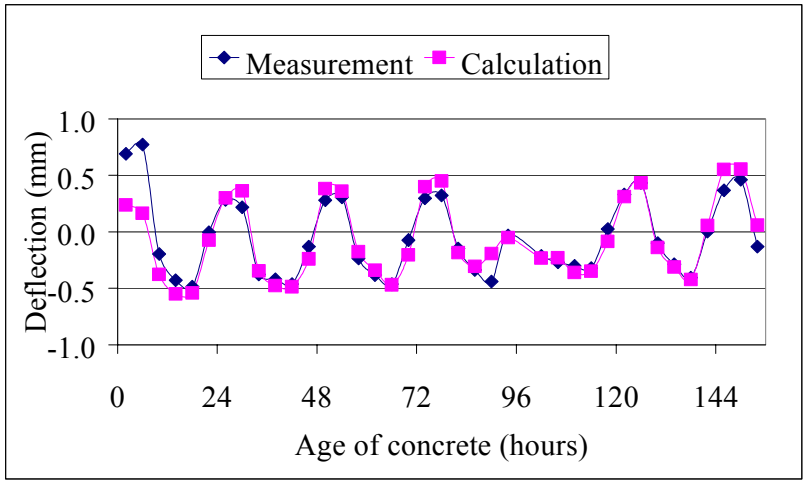

Figure 10 Comparison between Measured and Calculated Corner Deflection.

CONCLUSION

An approach of using the knowledge of heat and mass transfer for the prediction of temperature and relative humidity profile in a concrete slab was developed. It has been found that both the temperature and moisture changes in a concrete slab in the first few days after the concrete is placed are the main causes of restraint stresses and various distresses and therefore influence the quality of concrete over its lifetime.

A two-dimensional finite element program TMAC^2 has been developed to predict the temperature and relative humidity distributions due to specified environmental conditions. The temperature and relative humidity profile prediction was partially validated through the prediction of behavior of concrete slab such as corner deflection. A test slab was constructed and instrumented to collect slab temperature and relative humidity data to verify the availability of TMAC^2 program. On the whole, the predicted moisture and temperature profiles correspond to the measured data well.

Corner deflection of the test slab was measured carefully and compared to the results from the Westergaard's solution to show an example of a consistent analysis and design procedure of a concrete slab using predicted temperature and relative humidity profile from TMAC^2. The measured corner deflection agreed with the calculated corner deflection well and it explains that the TMAC^2 program is partially validated to provide more accurate predictions of behavior and distress of concrete slab.

REFERENCES

1. Neville, A.M. *Properties of Concrete.* 4th edition, John Wiley & Sons, Inc., New York, 1996.
2. Barnes, P., ed. *Structure and Performance of Cements.* Applied Sciences Publishers, New York, 1983.
3. Copeland, L.E., and Hayes, J.C. *The Determination of Non-Evaporable Water in Hardened Portland Cement Paste.* Bulletin 194. ASTM, Philadelphia, 1953, pp. 70-74.
4. Powers, T.C. *A Discussion of Cement Hydration in Relation to the Curing of Concrete.* Bulletin 25. Portland Cement Association, Skokie, Illinois, 1948, pp. 1-9.
5. Wang, L. *Early Age Characterization of Concrete Temperature and Moisture Parameters.* Ph.D. Dissertation, Texas A&M University, College Station, 2000.
6. Incropera, F.P. and DeWitt, D.P. *Fundamentals of Heat and Mass Transfer.* 4th edition, John Wiley & Sons, New York, 1996.
7. Klemens, P.B. *Theory of the Thermal Conductivity of Solids.* In R. P. Tye, Ed., Vol. 1, Academic Press, London, 1969.
8. Bazant, Z.P. and Najjar, L.J., *Nonlinear Water Diffusion in Nonsaturated Concrete.* Materials and Structures (RILEM), Vol. 5, No. 25, 1972.
9. Linsley, R.K., Kohler, M.A., and Paulhus, J.L. *Hydrology for Engineers.* 2nd edition, McGraw-Hill, New York, 1975.
10. Mohamed, A.R. and Hansen, W. *Effect of Nonlinear Temperature Gradient on Curling stress in Concrete Pavement.* Transportation Research Record 1568, Transportation Research Board, Washington D.C., 1996, pp. 65 - 71.
11. Wang, L. and Zollinger, D.G. *A Mechanistic Design Framework for Spalling Distress.* Transportation Research Record 1730, Transportation of Research Board, Washington D.C., 2000, pp. 18-24.